X-1

FLIGHT REENTRY EXPERIMENTS

by

Herbert A. Wilson, Jr.

and

Robert L. Wright

NASA - Langley Research Center

INTRODUCTION

Reentry technology has long depended on the simulation provided by wind tunnels, shock tubes, arc jets, and a variety of other ground facilities to advance the experimental verification of the results predicted from theory or postulated empirically from previous tests. As the application of information thus obtained approaches the point of application to the design of flight systems, the question of the extent to which the information can be applied with confidence inevitably arises. Sources of uncertainty are the assumptions necessary to obtain theoretical solutions, the inadequacy with which the complex reentry environment can be totally simulated on the ground, and the question of how well the ground facility results have been validated by flight comparisons. Thus the value of flight reentry testing is greatest when the tests either explore the nature of a phenomenon, difficult or impossible to simulate on the ground, or provide the validation for use of a system or concept developed from ground-based research.

The discussion presented outlines the current activity in flight reentry research at the Langley Research Center in terms of the techniques being used in a number of flight projects to investigate reentry environment, radio attenuation, materials behavior, and observable phenomena.

Several of the other papers given in these proceedings have highlighted some of the difficulties of simulating flight reentry phenomena in ground facilities. These center mainly on the size of the model that can be tested, the duration of the test, and the level of the variables determining heating rate. Virtually all ground facilities make compromises in at least one of these significant variables. The nature of these compromises is defined in figures 1, 2, and 3. Typical Mach number-altitude corridors for ballistic and lifting reentry bodies currently of interest are shown in figure 1. In figure 2, the capabilities of the so-called "cold" hypersonic facilities are superimposed on the reentry corridors. These facilities (most notably the 22-inch helium tunnel) cannot match the stream enthalpy, therefore are limited as to heating input, but can provide high Mach number basic fluid dynamics data. Capabilities of the "hot" hypersonic facilities are shown overlaid on the same reentry corridors in figure 3. These facilities give a reasonable simulation at low velocity, but for increasing flow velocity, they generally tend to fall off in their simulation of the heating. One exception is the expansion tube which suffers the characteristic difficulty of shock-type facilities in that the experiment time is small, that is, milliseconds or microseconds instead of minutes.

FLIGHT-TEST IMPLEMENTATION

A reentering body, generally speaking, first meets the atmosphere at a high altitude and a high velocity and slows down as it penetrates the atmosphere. Typical flight-test trajectories and the atmospheric environment they traverse are shown in figure 4. The trajectories shown are the Scout R-4 and ST-8 reentries. The hashed area indicates a proposed materials test at 40,000 fps. All of the vehicles to be discussed later fly trajectories similar to these, with the exception of the RAM (Radio Attenuation Measurements) vehicle, which flies a straightaway trajectory (not shown) with all data obtained on ascent.

This figure also indicates several conditions, such as oxygen dissociation, nitrogen dissociation, and ionization which characterize the environment in different regimes and account for a variety of different aerodynamic and flow-field effects. The region of the flight environment of greatest concern at the present is indicated as the Apollo Reentry Envelope and the current programs for obtaining data in this envelope will be discussed later.

Launch Vehicles

Flight programs are often identified in terms of the launch vehicle which may be misleading. Actually, the vehicles exist to support the program, and not vice versa, but vehicle nomenclature does in many cases provide a convenient reference to the program. The launch vehicles currently being used are shown in figure 5. The four-stage Pacemaker vehicle is a low-cost vehicle capable of speeds of the order of 14,000 to 16,000 feet per second. Its use enables low-cost flights for preliminary exploratory work, and for flights providing some overlap with ground facilities.

The payload capability of the Pacemaker is approximately 40 pounds. The RAM B vehicle is capable of boosting 200 pounds on a straightaway, ascending trajectory to a velocity of approximately 18,000 feet per second. The Trailblazer vehicle, used mainly in the field of reentry observables, imparts extremely high velocities (34,000 feet per second) to payloads on the order of 5 grams when equipped with a shaped-charge gun as a last stage.

The workhorse for our heavily instrumental payloads is the Scout vehicle which is used in both the four-and five-stage configurations. Reentry velocities and payload weights of 26,000 feet per second and 200 pounds, respectively, have been attained with the four-stage configuration and 28,000 feet per second and 150 pounds in the five-stage configuration. A photograph of the five-stage Scout vehicle in the launch tower is shown in figure 6. It should be noted that everything forward of the third stage is covered with a heat shield. Figure 7 shows a typical five-stage Scout reentry, in this case the ST-8 heating and environmental test which will be discussed in detail later. Launched from Wallops Island, the flight plan called for two stages firing upward and three downward or reentry-firing stages. A peak velocity of 22,500 feet per second was achieved with impact southeast of Bermuda.

A recent development is the Project Fire vehicle which consists of the Atlas-D boosting a second-stage X-259 motor equipped with a guidance and control system and a 200-pound spacecraft (fig. 5). The second-stage rocket and the guidance and control systems are adapted from the Scout vehicle. The Fire vehicle is capable of a reentry velocity of approximately 38,000 feet per second.

Data Acquisition

The spacecraft used with the launch vehicles just described are

tailored to the particular program requirements. A key factor in each spacecraft is the selection of the sensors, transducers, and other data acquisition system components. A summary of the measurements and sensor selection for the Fire Project Reentry spacecraft is shown in figure 8. Figure 9 shows a block diagram of the instrumentation for a typical spacecraft for monitoring and transmitting the transducer data. Such data as temperature measurements are usually commutated, while pressures and accelerations are measured continuously. The telemetry system provides for broadcasting data in real time through one transmitter and antenna system. Inasmuch as the reentering spacecraft experience communications blackout, it is necessary to circumvent this problem with a delay train. A delayed tape unit with a delay long enough to last through the blackout period stores these data until the vehicle has slowed to less than 10,000 feet per second. At this time, all of the measurements that occurred during reentry are rebroadcast until impact. This technique has been very useful and is used on all of the five-stage Scout reentry shots and the Fire Project.

With a recoverable system, an onboard recoverable recorder will provide additional redundancy. On the Pacemaker vehicle, a recovery system was developed, consisting of a sequence of drogue-chutes and parachutes to provide a gradual descent into the ocean. Beacons provide locations aids for rapid recovery and all the data are obtained from the onboard recorder. This recovery technique system is indicated in figure 10.

FLIGHT-TEST PROGRAMS

The preceding sections have reviewed the test conditions that can

be simulated by ground facilities and flight tests, and outlined flight-test implementation in terms of available launch vehicles and methods of data acquisition. With this material as a background, the role of simulation in flight reentry experiments can be determined by looking at the details of some specific flight programs. The flight programs to be discussed deal with investigations of one or more of the following problem areas:

(1) Environmental (heating);

(2) Materials response;

(3) Communications problems; and

(4) Observables.

These categories are essentially areas of interest which will provide basic data for determining design parameters and trade-offs in the design of a full-scale spacecraft that must reenter the earth's atmosphere, such as Apollo or future interplanetary exploration vehicles.

Environmental

The first environmental spacecraft to be discussed is the Scout ST-8 reentry package. A photograph of the spacecraft is shown in figure 11. Spacecraft components and pertinent dimensions are presented in figure 12. The chief feature of the environmental payload is the inconel nose cap calorimeter, whose purpose was to provide quantitative total heat-transfer information during the first 15 seconds of reentry. Beneath the inconel nose cap was a teflon nose cap to protect the spacecraft and instrumentation package. Ablation sensors were mounted on the front of the nose cap to provide further information on the heating during the later part of the reentry. A canister contained the instrumentation, including the delay train system described earlier, with the actual structure of the vehicle afterbody serving as the antenna.

The sequence of events during reentry is indicated on the velocity-altitude diagram in figure 13. Low-level calorimeter heating data were obtained above 300,000 feet. The prime heating data occurred as the spacecraft descended from 300,000 to 200,000 feet, where the inconel cap melted. After the inconel nose cap melted, the ablation sensors in the teflon nose cap provided overall measurements of the ablation recession due to total heat input. A typical temperature history obtained during the prime heating period is shown in figure 14 to indicate the good quality of the data obtained from the flight.

A further step in investigation of hypervelocity environment has been undertaken by the Fire Project which has primary emphasis on the heat-transfer process at lunar return velocity of about 38,000 feet per second. Figure 15 is a representation of the total heat pulse and radiative heat pulse that would occur for a reentry at 37,000 to 38,000 feet per second. At this velocity, the total heat is predominately convective, but the speed is sufficiently high for the radiative heating to become appreciable. At the outset of the Fire Project, there was considerable speculation on whether or not this radiative heating had a large input due to nonequilibrium. A primary part of the Fire objective was to evaluate the nonequilibrium radiation. Since then, however, estimates of nonequilibrium heating indicate the problem to be considerably less serious than expected. Nevertheless, a major objective of the Fire Project was the determination of the total heating at high speeds and, in particular, the division of the total heating between radiation and convection.

To facilitate this objective, total heat transfer was measured by means of a rather complex succession of metal calorimeters on the front of the spacecraft using thermocouples as sensors. Hot gas radiation was

measured through windows in the stagnation region, at the shoulder of the body, and in the afterbody. Spectral measurements were made at the stagnation location and total radiometers were provided at all three windows. Materials response (regression rates) and radio attenuation information was also obtained.

The Project Fire reentry package and its supporting structure (the conical adaptor on top of the last-stage motor) can be seen in figure 16. The reentry package, similar in shape to the Apollo, had three calorimeters which were designed to be effective at different times during the flight. The reason for using three calorimeters is illustrated in figure 17. It is obvious that a single calorimeter could not be designed to survive the entire flight. The total heat pulse curve shows that portion of the heat pulse for which each of the three calorimeters would provide data. An ablation material was placed between the calorimeters to protect the subsequent calorimeter until exposure. Therefore, with this sequence of calorimeters, enough of the total heating pulse curve could be obtained so that, with the aid of theory, the entire heat pulse curve could be determined. Figure 18 presents the mission profile and the major sequence of events in the Project Fire trajectory. Reentry at a velocity of 37,800 feet per second occurred in the vicinity of Ascension Island, 4500 miles downrange from Cape Kennedy, the launch site.

Figure 19 presents a summary of flight-test data available from aerodynamic heating environmental experiments. Most of the data have been obtained from blunt-nosed configurations. The Fire Spacecraft which was Apollo shaped and the other heating projects were mainly blunt nosed. However, many of the spacecraft that will fly in the future will not necessarily

be blunt-nosed bodies by any means. An experiment on which preliminary work is currently being performed, utilizes the long, slender and relatively sharp cone shown in figure 20. The objectives of the experiment are to determine turbulent heat-transfer results at a velocity of approximately 20,000 feet per second (approximately twice the speed for which any similar data are available). These results are important not only for long conical bodies, but for vehicles such as the space plane or any type of glide reentry vehicle which operates at a relatively high Reynolds number and depends on radiation heat transfer to dissipate some of its heat. Thus, this vehicle must be long (10 feet) and flown at relatively low altitudes for at least a portion of its trajectory to assure turbulent flow over the last part of the cone.

Materials Reponse

In the materials response area, as discussed earlier by Mr. Brooks, there have been diverse predictions made from the available ground test data. Flight tests therefore are useful for determining which predictions are most reliable. A sectioned view of a 3-inch-diameter specimen tested in an arc-heated facility is shown in figure 21. A section of a heat shield of the same material from a flight model which experienced a similar total heating history is seen in figure 22. It is evident that the char layer from the flight test is much thinner than that from the ground test.

In other cases, phenomena difficult to test on the ground can be investigated. Figures 23 and 24 show the results of a flight test to determine possible effects on heat shield behavior of meteorite damage before reentry. The flat-faced model, roughly 6 inches in diameter, is shown in figure 23 before flight. Three ablation sensors were mounted

across the front face and a 1/4-inch-diameter hemispherical crater was located approximately 1 1/2 inches from the stagnation point. A second indentation, simulating meteorite damage, is seen on the cylindrical portion of the spacecraft. The spacecraft was test flown on the Pacemaker vehicle and recovered. Figure 24 shows the damage resulting from the change in the flow field caused by the simulated meteorite damage.

The prime objective of the Scout R-4 experiment, flown August 18, 1964, was to provide a real environment test of a candidate material for the Apollo heat shield to verify test work done in ground facilities. As the spacecraft and experiment were discussed fully in the presentation by Mr. Brooks, no further discussion is considered necessary.

Communication Problems

The communications blackout or attenuation of radio signals due to the ionizing sheath around a spacecraft during reentry is currently being investigated by the RAM (Radio Attenuation Measurements) program. Figure 25 indicates the velocity regimes for various ionization reactions, including molecular, atomic, photo and electron-impact ionization. Also noted in the figure are the regimes investigated by the RAM flight tests. RAM A and B flights have produced good measurements of the attenuation for VHF C-band and X-band frequencies in the molecular ionization range with straightaway or ascending flights. A considerable amount of work has also been done in this regime with ICBM tests. Proposed RAM C flights will investigate the velocity band where atomic ionization is fully developed. Future tests will measure the blackout region for flight velocities above 30,000 feet per second.

A diagram of the RAM C spacecraft is shown in figure 26. The spacecraft is 20 inches in diameter at the base, 38 inches long, and weighs

several hundred pounds. The important things to note on the diagram are the VHF, C-band, and X-band antenna systems with the associated telemetry equipment.

Figure 27 presents the C-band and VHF blackout regions. The boundaries were established with a combination of the theory and flight tests. RAM and Mercury trajectories from which some of these data were obtained are indicated on the figure as is the proposed Apollo trajectory.

Observables

NASA and the Smithsonian Astronomical Observatory are currently engaged in a joint project whose purpose is to create artificial meteors. The objectives of this project are found in figure 28.

Trailblazer I and II vehicles were used to impart reentry velocities of approximately 34,000 feet per second to a simulated meteor. A 5-inch-diameter rocket motor was mounted atop the four-stage vehicle. A shaped-charge accelerator was connected to the fifth-stage spherical motor as shown in figure 29. After burnout of the fifth stage, the shaped charge is detonated, compressing the spit-back tube into a pellet which is propelled through the inhibitor as an artificial metoer at extremely high velocity. The velocity, deceleration, light intensity, and spectra of the simulated meteor can be measured. Also, with the aid of ground test firings, pellets can be recovered and the mass and shape determined.

Thus, by injecting an artificial meteor of approximately known mass at a known velocity and at a location where observation stations have been placed, it is possible to calibrate observables for natural meteors to determine more accurately the luminous and ionization efficiency.

A typical meteor reentry flight profile is shown in figure 30. The first two stages fire upward to attain an altitude of about a million feet

and the last three stages and shaped-charge accelerator fire downward to impart the needed reentry velocity. Launched from Wallops Island, the pellet impacts some 100 nautical miles downrange, making the east coast from Wallops to Hatteras available for setting up optical and radar observation sites. Other meteor simulation tests, using two-stage Nike-Cajun vehicles with the shaped-charge accelerator, have produced reentry at lower velocities to provide luminous efficiency data over a range of reentry velocities. Figure 31 shows some results of the Meteor Simulation Project. The theory of Öpik, developed in 1958, for the luminous efficiency of meteors is indicated for a range of reentry velocities.

CONCLUDING REMARKS

The foregoing discussion has shown the way in which flight testing supplements, extends, and reinforces the usefulness of data from ground test facilities. Flight tests can provide an anchor point in evaluating ground test data. Although flight tests can avoid some of the inherent problems of ground facilities, they are expensive, putting a premium on each test to provide the most data that can be acquired.

The portions of the reentry flight spectrum which can be simulated by "hot" and "cold" ground facilities are reviewed and some of the current flight programs for obtaining data in the Apollo Reentry Envelope are discussed. The programs are categorized as to (1) environment (heating), (2) materials response, (3) communication problems, and (4) observables. A discussion of the launch vehicles, unknown parameters, and methods of data acquisition for each program is presented.

X-13

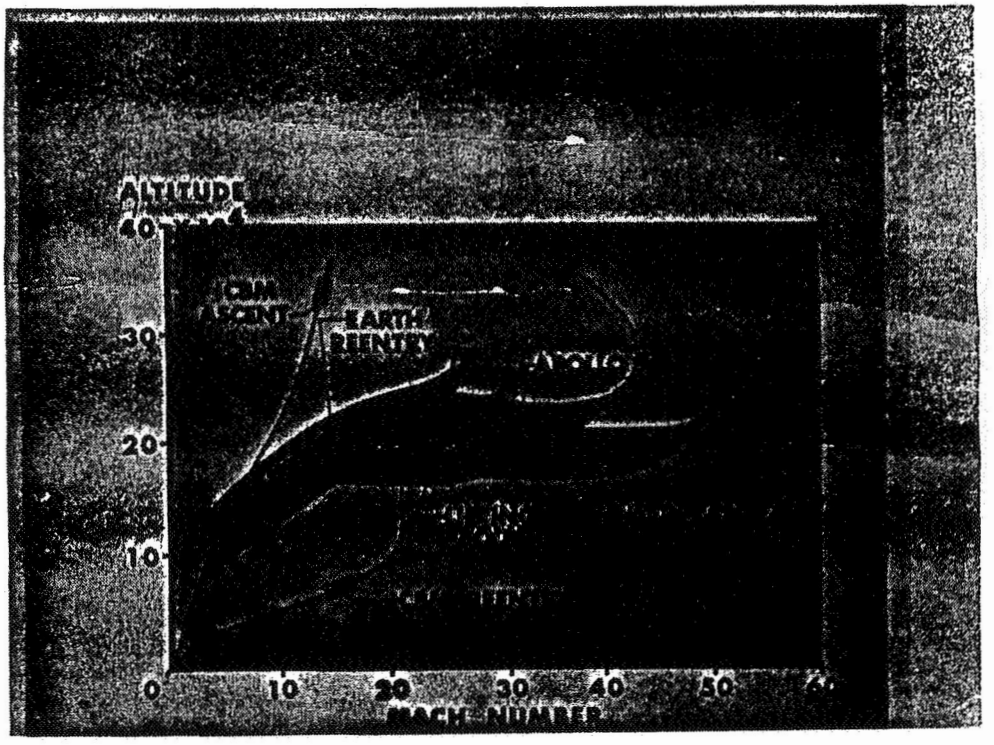

NASA

Figure 1 Typical reentry corridors

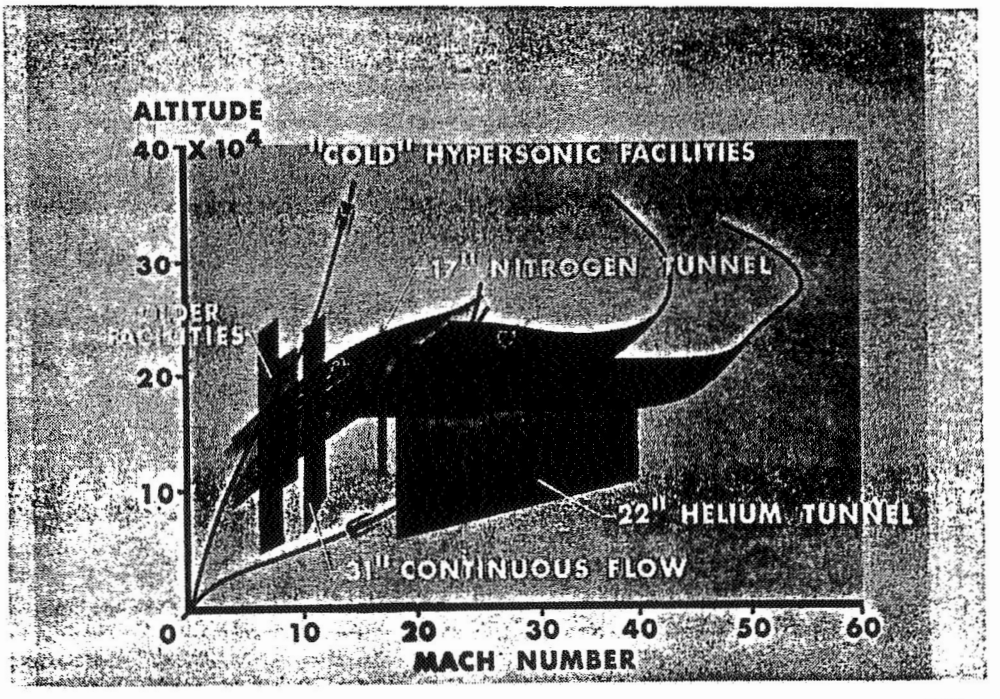

NASA

Figure 2 Capabilities of "cold" hypersonic ground-test facilities

X-14

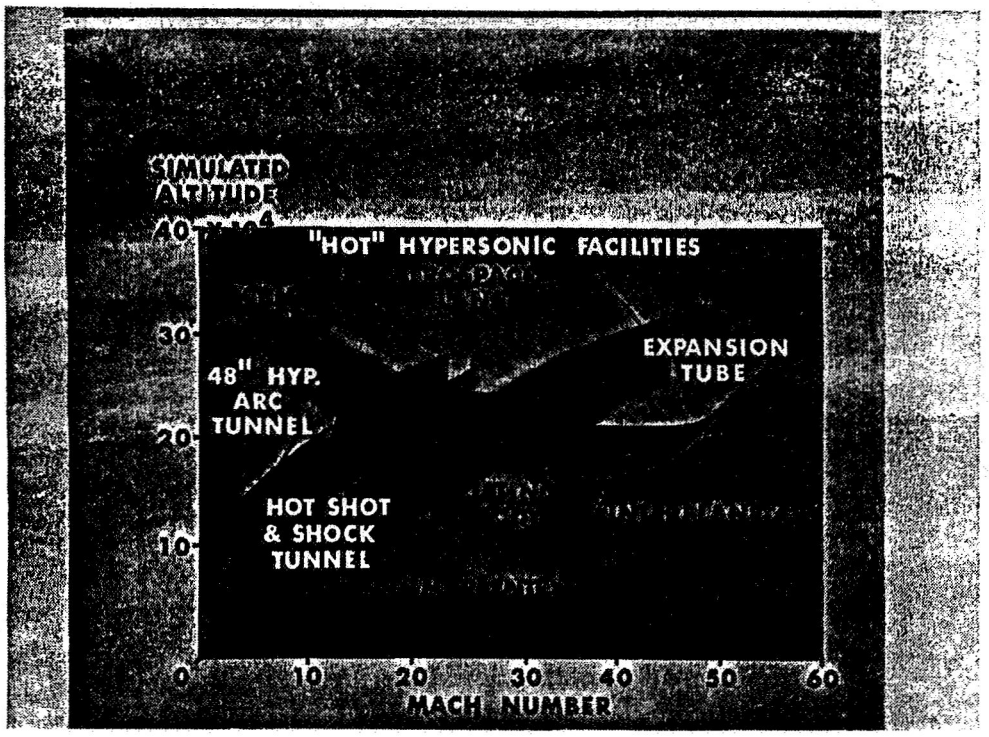

NASA

Figure 3 Capabilities of "hot" hypersonic ground-test facilities

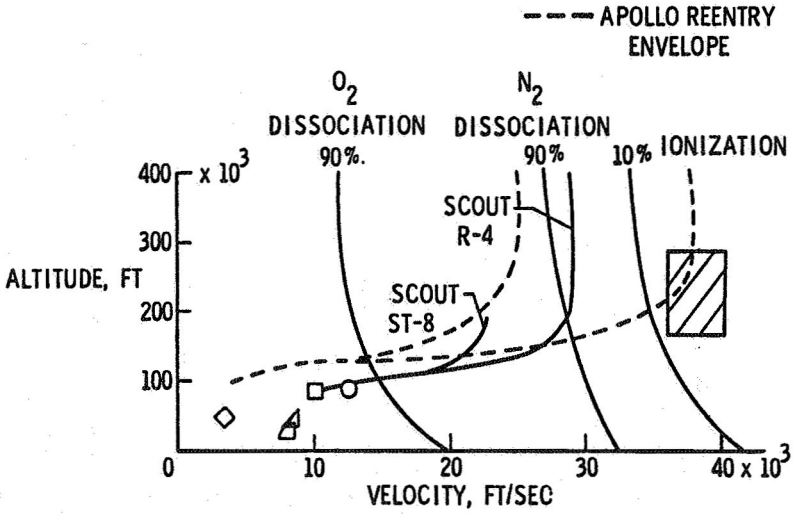

NASA

Figure 4 Typical flight-test trajectories and environment

X-15

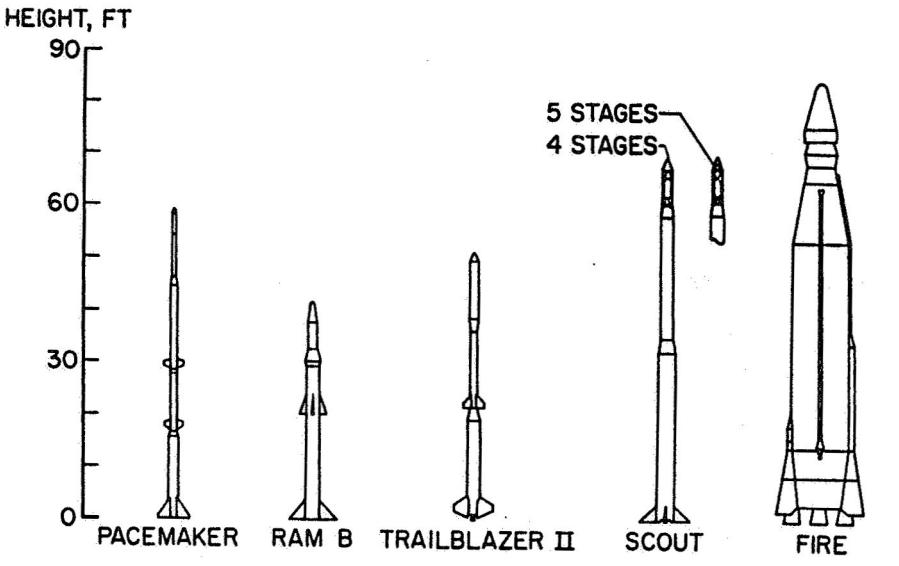

NASA

Figure 5 Reentry launch vehicles

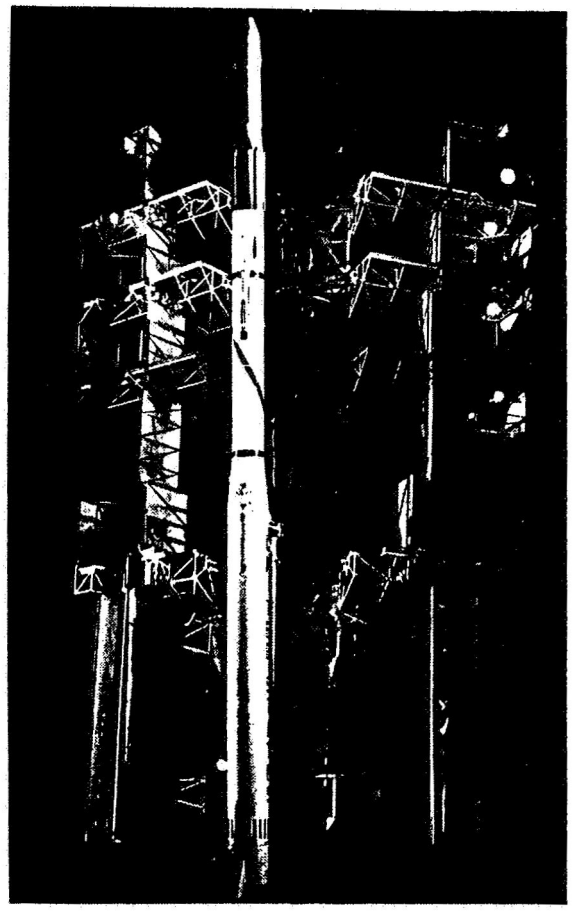

NASA

Figure 6 Five-stage Scout vehicle in launch tower

X-16

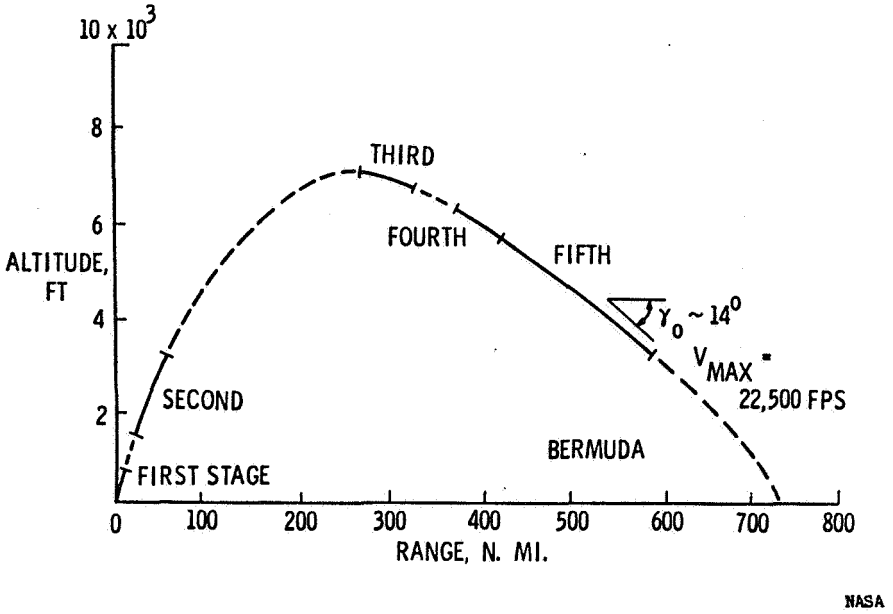

Figure 7 Typical Scout reentry trajectory

RESEARCH MEASUREMENTS

MEASUREMENT	METHOD	SENSOR
TOTAL HEAT TRANSFER	METAL CALORIMETERS	THERMOCOUPLES
HOT GAS RADIATION	WINDOW AND RADIATION SENSOR	TOTAL AND SPECTRAL RADIOMETERS
MATERIALS RESPONSE	REGRESSION RATE	THERMOCOUPLES STEPPED IN DEPTH
RADIO ATTENUATION	ANTENNA CHARACTERISTICS	VSWR, IMPEDANCE, AND SIGNAL RECEPTION

Figure 8 Research measurements and sensors

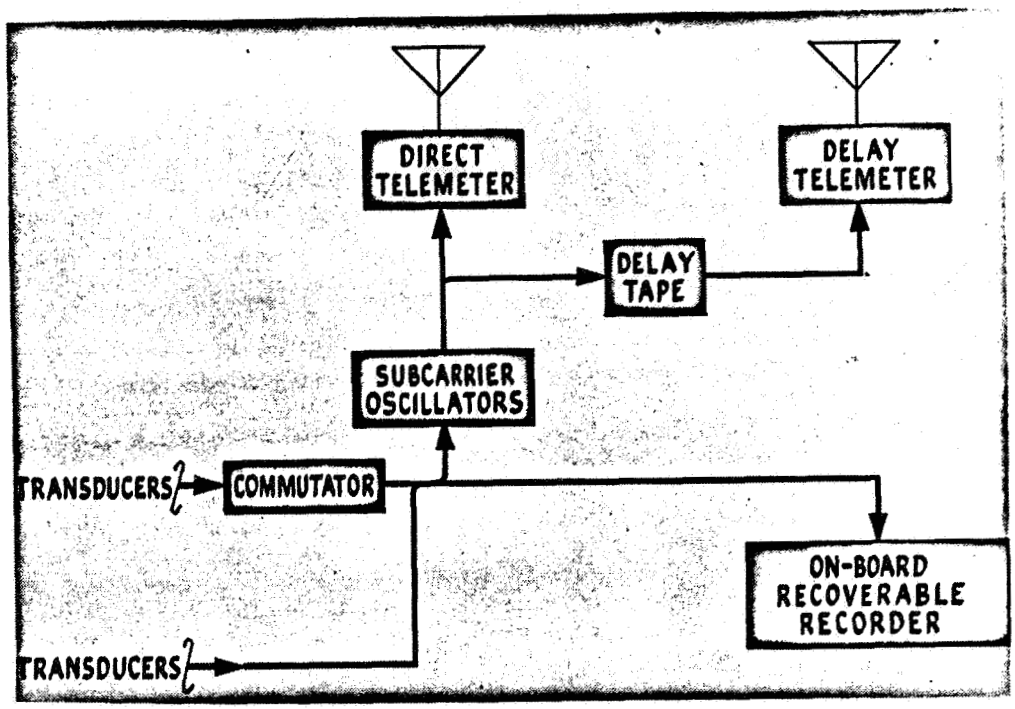

NASA

Figure 9 Data acquisition instrumentation

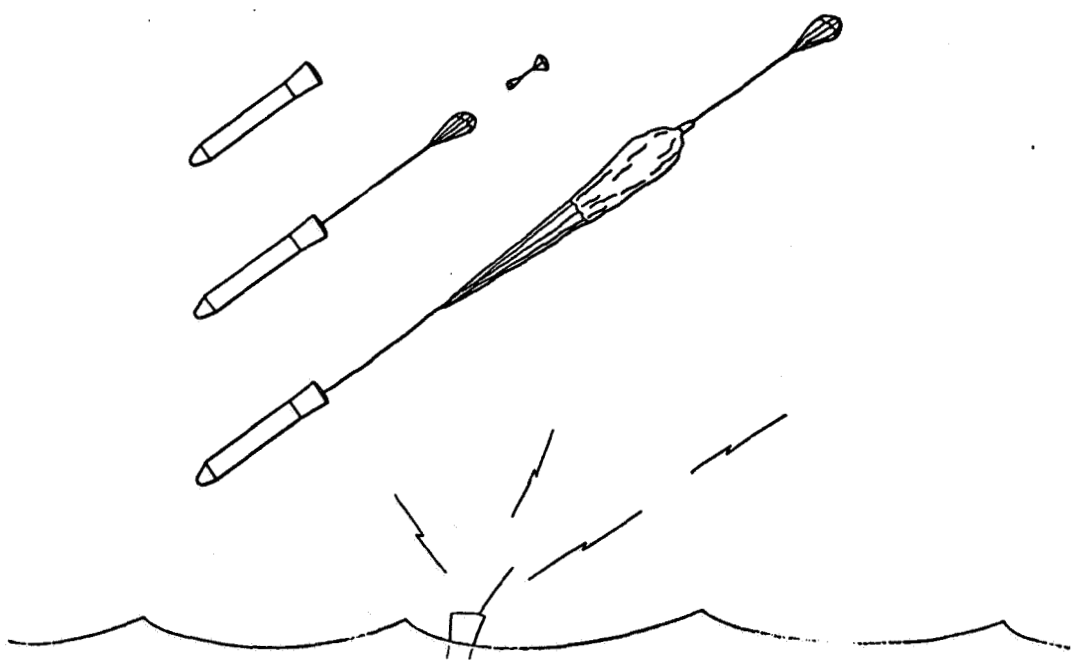

NASA

Figure 10 Spacecraft recovery system

X-17

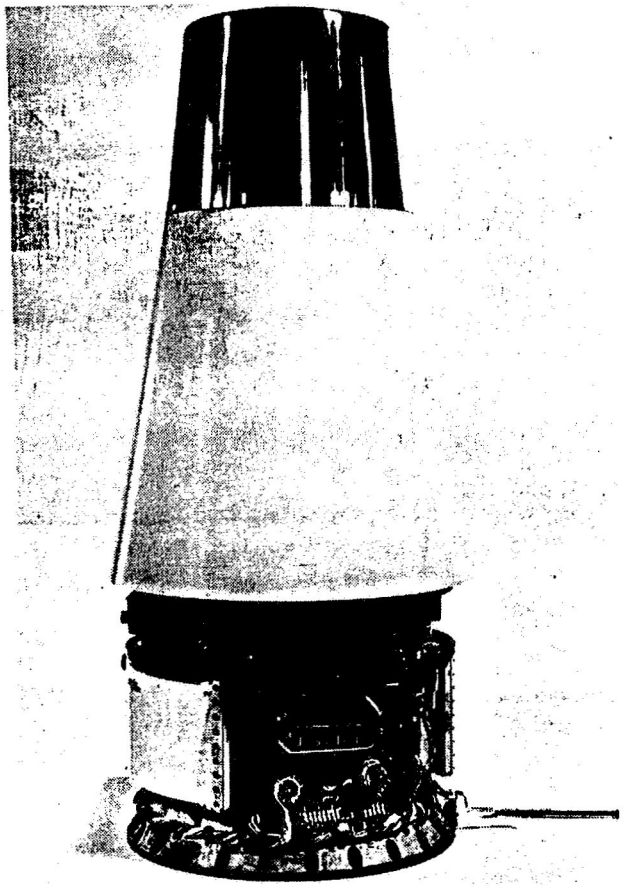

Figure 11 Scout ST-8 reentry package

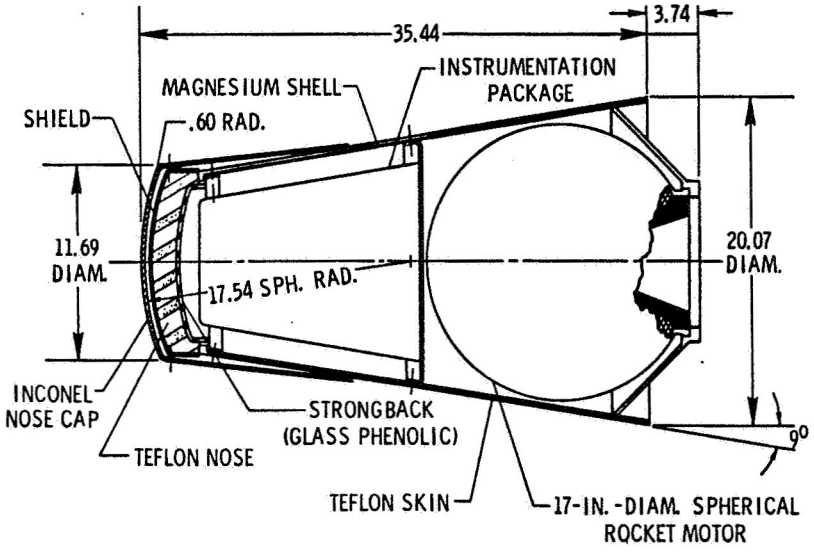

Figure 12 Scout ST-8 components

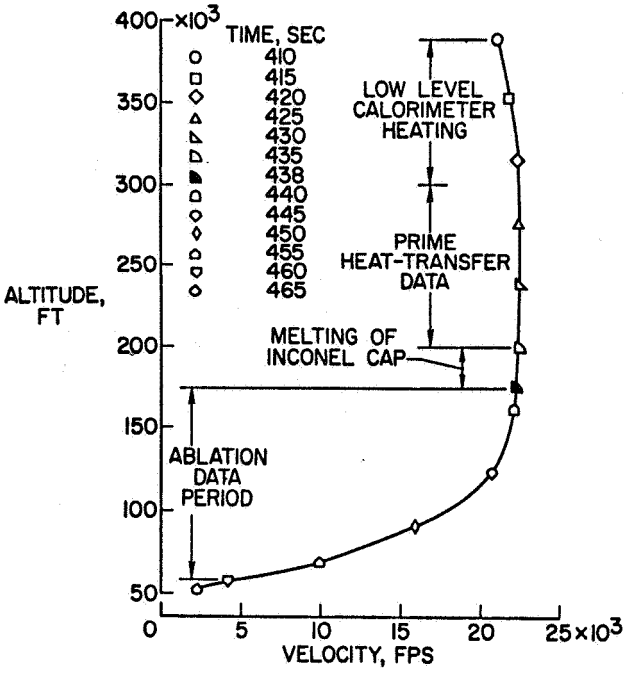

NASA

Figure 13 Sequence of events during ST-8 reentry

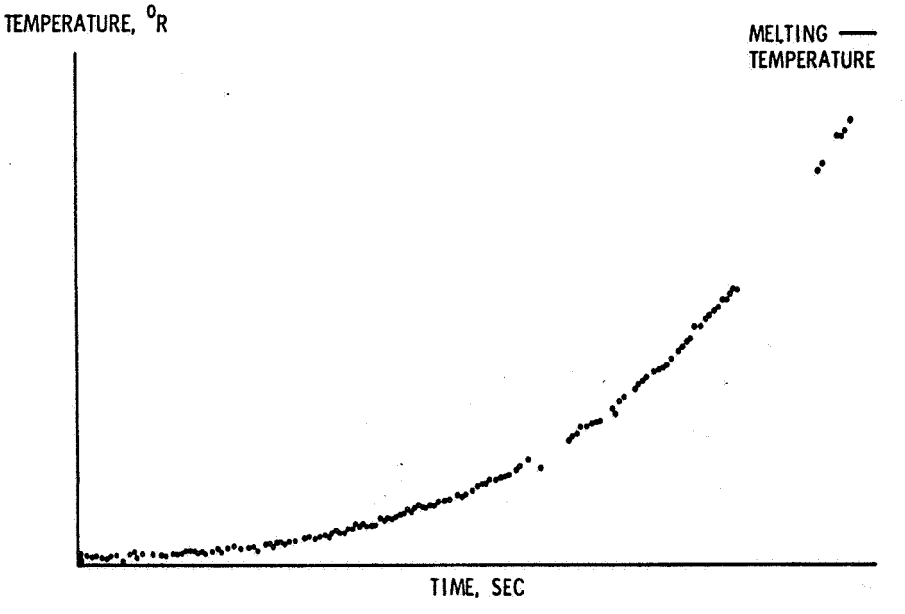

NASA

Figure 14 Typical temperature history during prime heating period

SCHEMATIC HEATING TIME HISTORIES

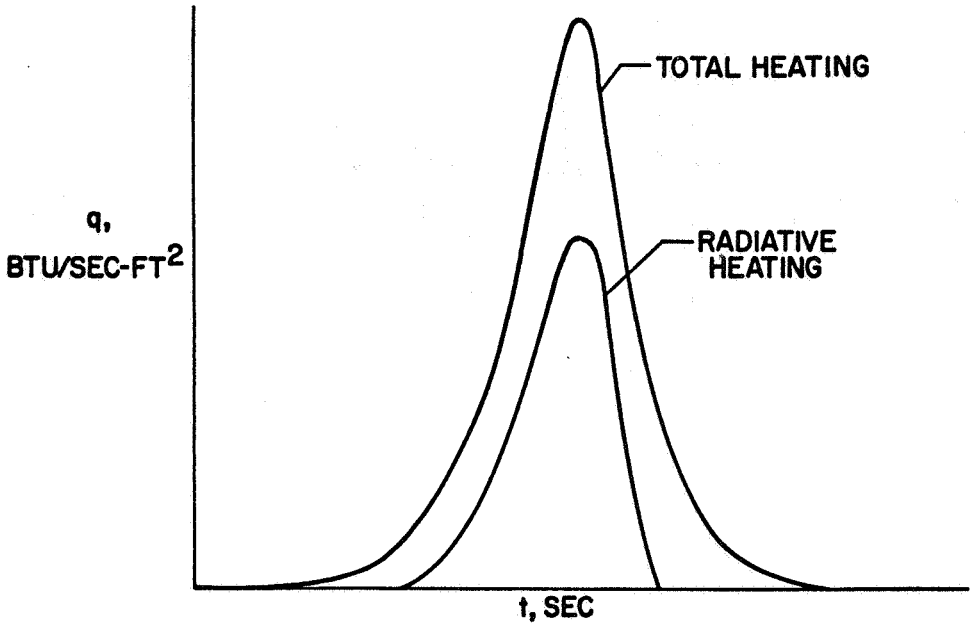

Figure 15 Approximate total and radiative heat pulses for a 38,000 fps reentry

PROJECT FIRE REENTRY PACKAGE

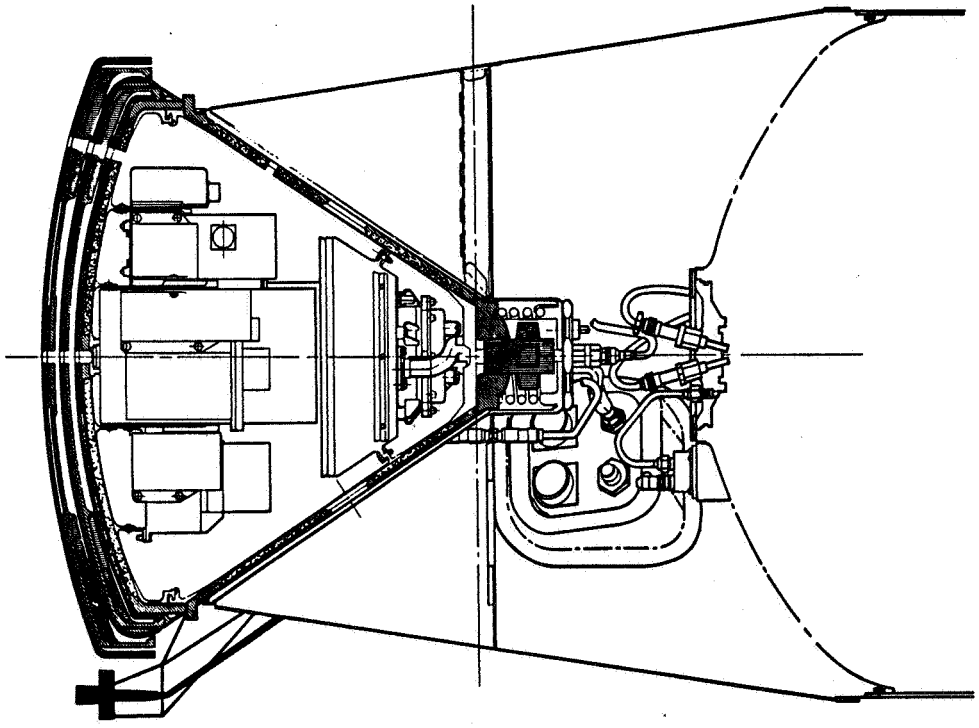

Figure 16 Project Fire reentry package and supporting structure

X-21

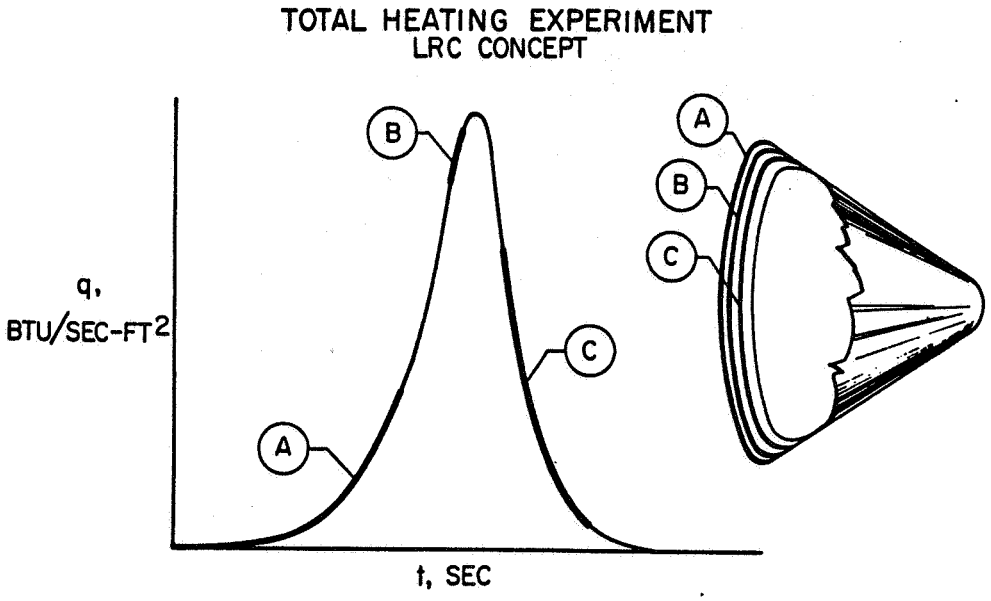

Figure 17 Portions of the heat pulse for which each calorimeter provided data

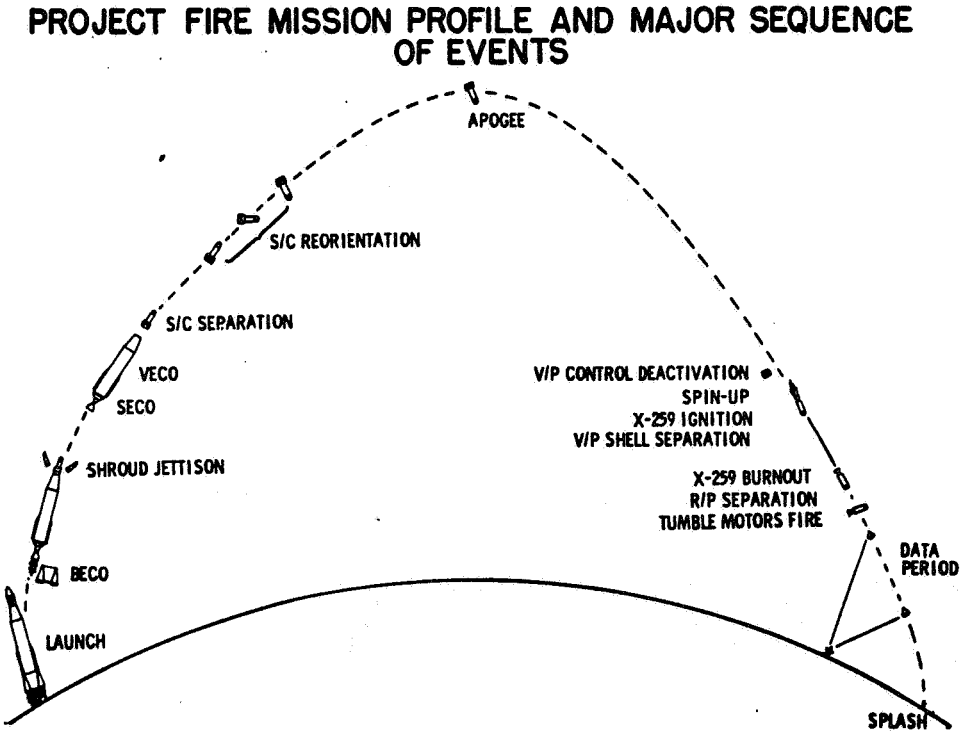

Figure 18 Project Fire mission profile and sequence of events

X-22

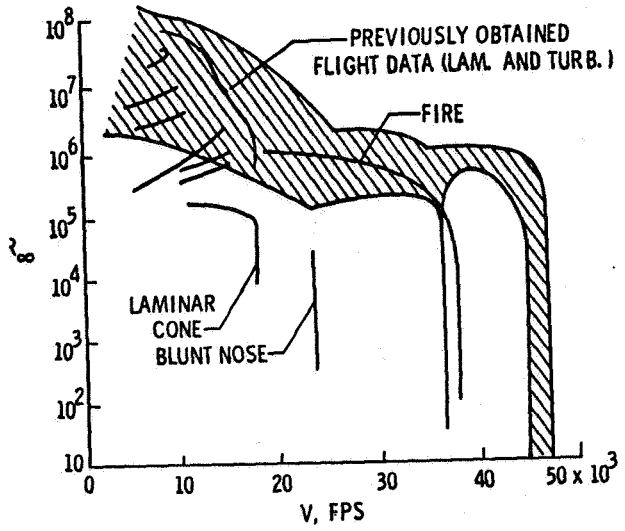

NASA

Figure 19 Summary of flight-test testing data

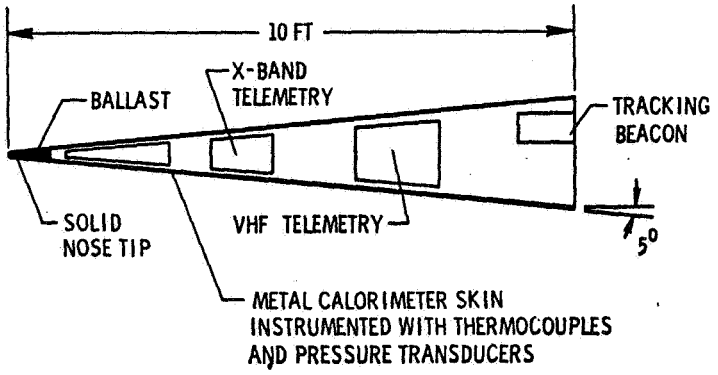

NASA

Figure 20 Turbulent heat-transfer experiment spacecraft

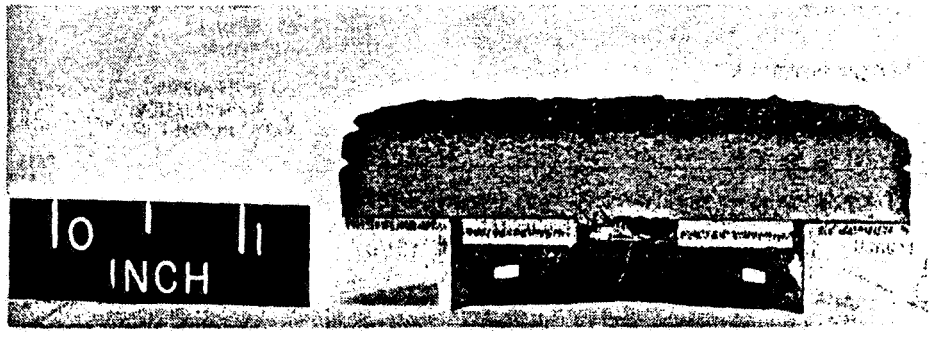

NASA

Figure 21 Ground-test ablation simulation specimen

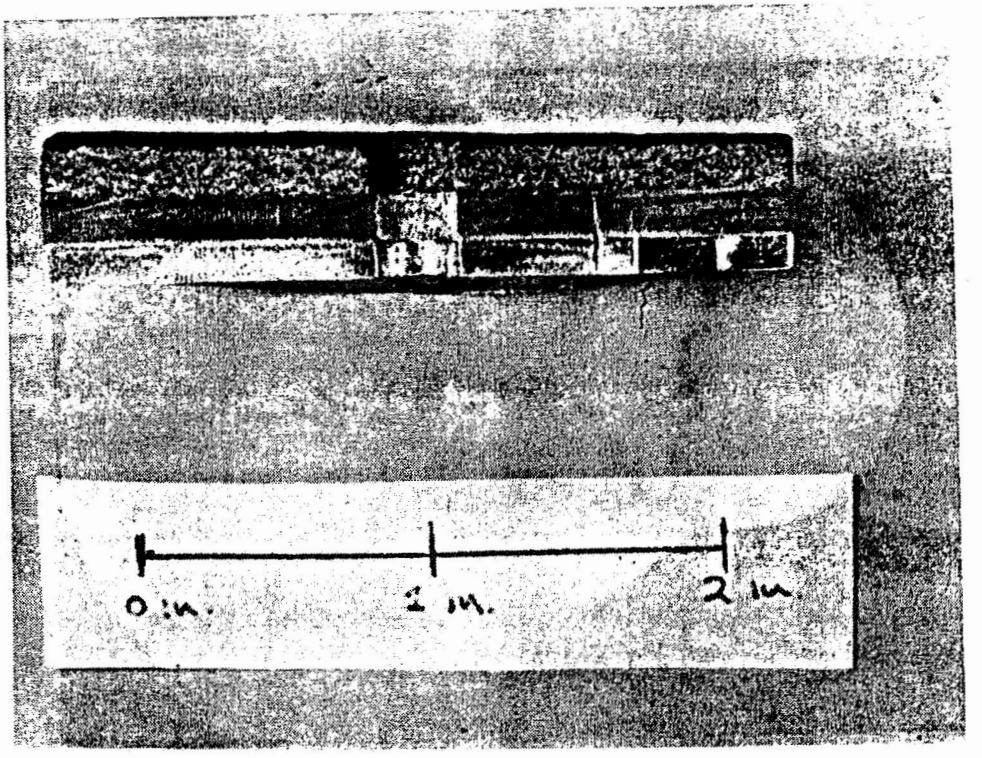

NASA

Figure 22 Flight-test ablation simulation specimen

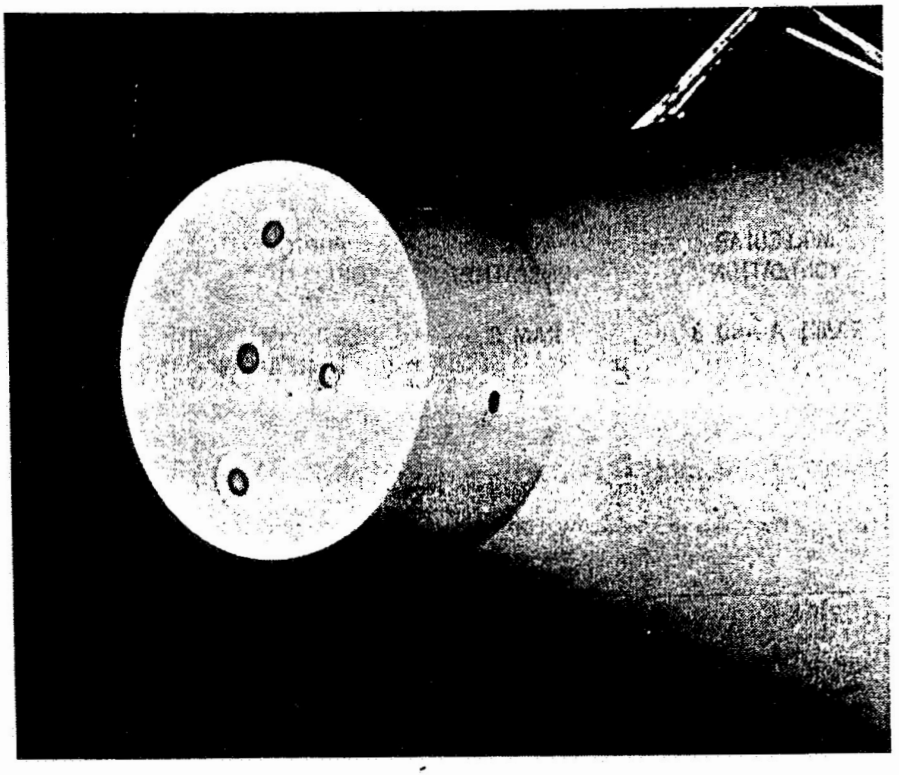

NASA

Figure 23 Meteorite damage ablation model before flight

X-24

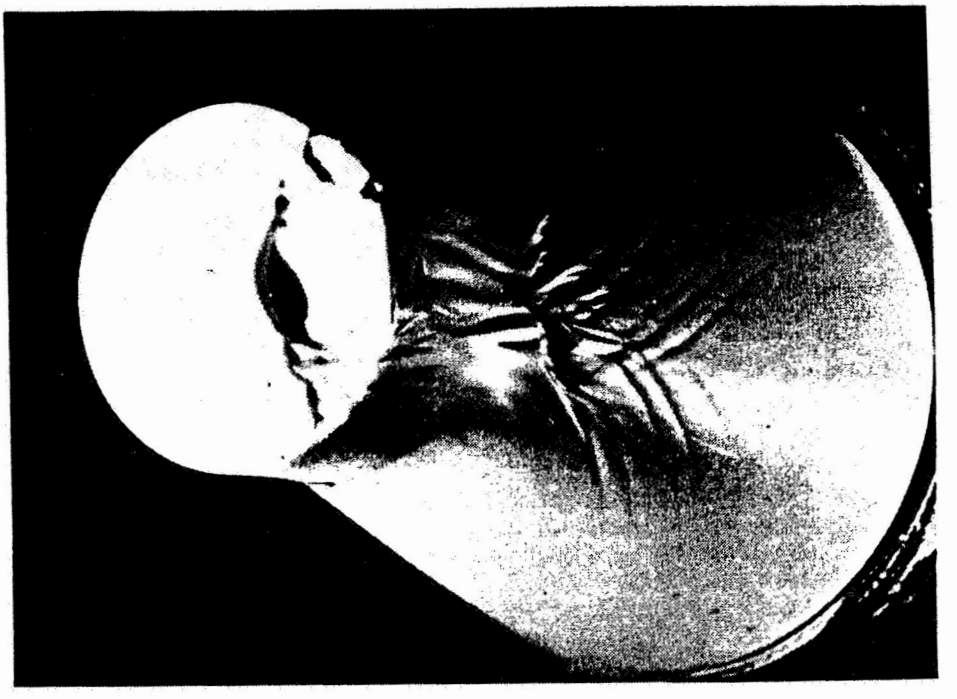

NASA

Figure 24 Meteorite damage ablation model after flight

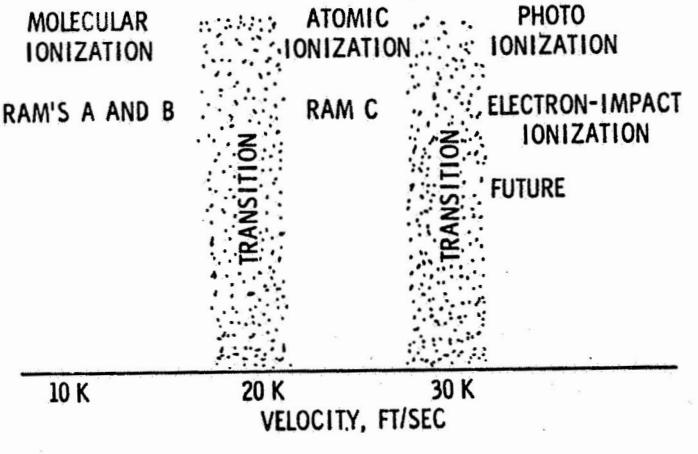

NASA

Figure 25 Velocity regimes for ionization reactions

X-25

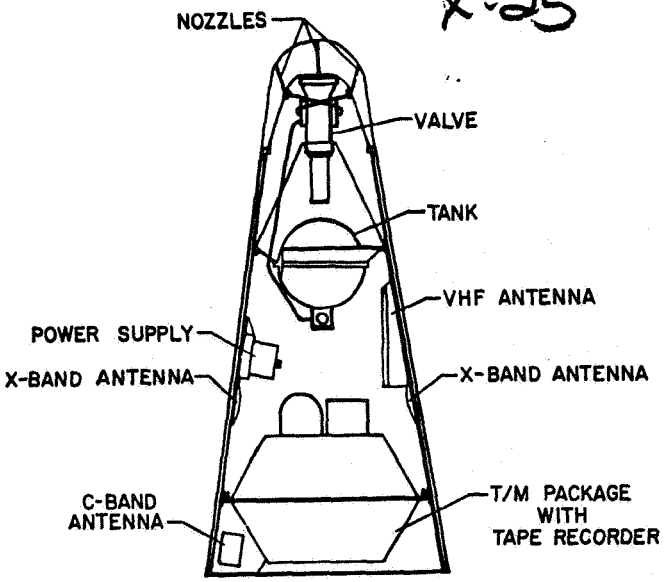

NASA

Figure 26 RAM spacecraft

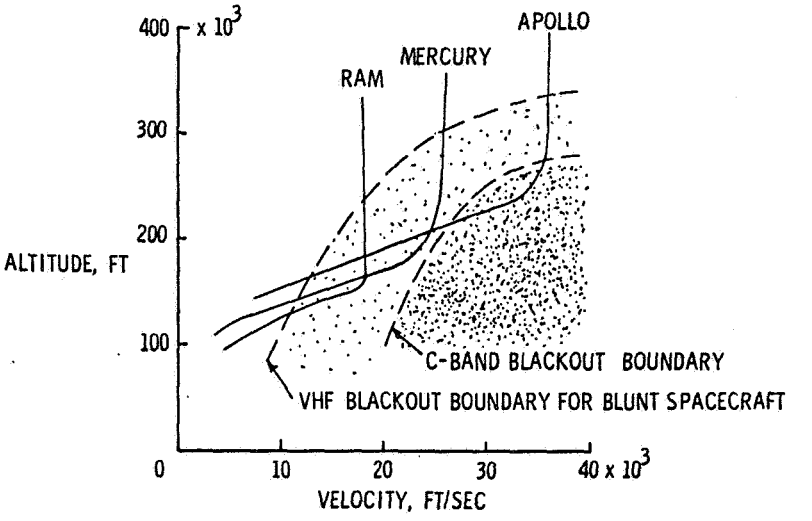

NASA

Figure 27 VHF and C-band blackout regions

OBJECTIVES:

1. CALIBRATE THE OBSERVABLES FOR NATURAL METEORS
   (a) BY OPTICAL MEASUREMENTS
   (b) BY RADAR MEASUREMENTS
2. DETERMINE TWO KEY COEFFICIENTS IN THE PHYSICAL THEORY OF METEORS FOR EACH OF THE PREDOMINANT METALS FOUND IN NATURAL METEORS
   (a) LUMINOUS EFFICIENCY, $\tau = \frac{\text{LIGHT ENERGY}}{\text{KINETIC ENERGY}}$
   (b) IONIZATION EFFICIENCY, $\tau_q = \frac{\text{IONIZATION ENERGY}}{\text{KINETIC ENERGY}}$
3. REENTER PURE METALS AT 10 TO 25 KM/SEC
   (a) ROCKET VEHICLES
   (b) SHAPED CHARGES

NASA

Figure 28 Meteor simulation project objectives

X-26

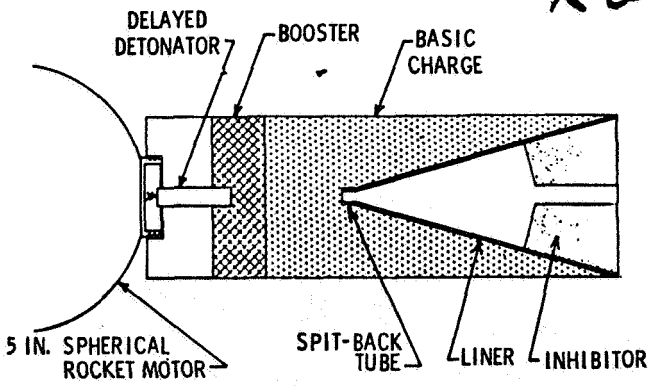

NASA

Figure 29 Shaped-charge accelerator

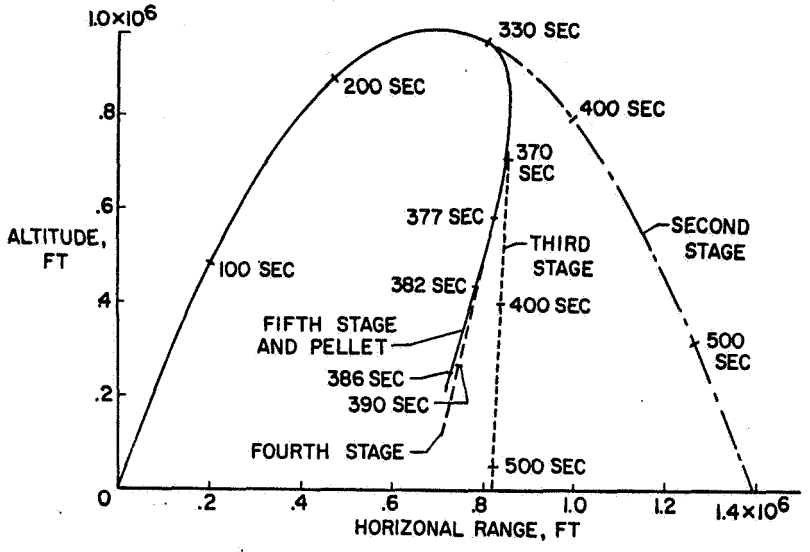

NASA

Figure 30 Typical simulated meteor reentry flight profile

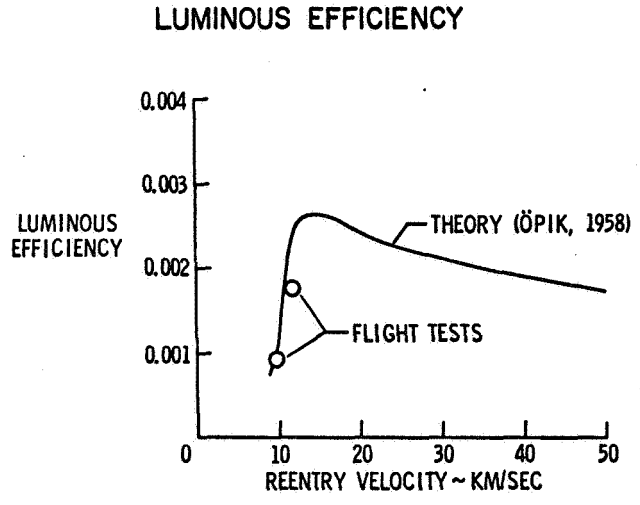

Figure 31 Luminous efficiency results